IP/BBSR/93-25

L-Shell Ionization studies of Pb and Bi with alpha particles

B. B. Dhal, T. Nandi and H. C. Padhi

Institute of Physics,Bhubaneswar-751005,India

31

Abstract

Absolute ionization cross-sections for the L-subshells of Pb and Bi by alpha particle bombardment(2.2-8.2MeV) have been determined from the measured data and the presently available radiative transition probabilities,fluorescence yields,and Coster-Kronig factors.The measured ionization cross sections and their ratios are compared with the results of ECPSSR calculations.The measured individual cross-sections for L_1 and L_2 subshells deviated in opposite directions from the theory ,whereas their sum shows good agreement.The L_3 and total ionization cross -sections obtained from the data also show good agreement with the ECPSSR theory.The ionization cross-section ratios $\frac{\sigma_{L_1}}{\sigma_{L_2}}$ and $\frac{\sigma_{L_3}}{\sigma_{L_2}}$ show large deviations from the ECPSSR theory,but they are in better agreement with the RPWBA-DHS-BC theory suggesting the importance of the electronic wave function of the target atom.The experimental X-ray production cross-section ratios are found to be in better agreement with the theoritical results obtained from using ECPSSR ionization cross sections and the decay yield data of Xu and Xu rather than those obtained from using the decay yield data of Krause.The absolute X-ray production cross-sections,however,are in better agreement with the theoritical results obtained from using the decay yield data of Krause.The measured centroid energy of the L_η lines of Pb shows large deviations at high projectile energy, whereas for Bi large deviations are found at the low energy region.

Fermilab Library
0 1160 0036278 4

IP-BBSR-93-25

I.Introduction

In an earlier paper[1] we presented our results on L-shell ionization studies of Pb and Bi for proton bombardment and in this work we present the results for alpha particle bombardment in the energy range of (0.5-2.0)MeV/amu.Although considerable efforts have been put in understanding the L-subshell ionization process[2-6] by heavy charged particles still the situation seems to be very fuzzy.The first study in Au for proton and alpha particle bombardment was reported by Datz et.al,[2] which showed significant deviation of the α particle data from the proton data at low energy.It also indicated deviations for L_1 subshell ionization cross sections and the cross section ratios $\frac{\sigma_{L_1}}{\sigma_{L_2}}$ and $\frac{\sigma_{L_3}}{\sigma_{L_2}}$ from both non-relativistic and relativistic PWBA theories[7]. After this work Chang et.al.[3,4] reported their work on L-subshell ionization for various heavy elements by alpha particle bombardment in which they showed for the first time that the low energy behaviour of the cross-section ratio $\frac{\sigma_{L_3}}{\sigma_{L_2}}$ is dependent on the outer electronic configuration of the target atom.However, their conclusion was refuted by the work of Li et.al[5],which did not show any target outer electronic configuration dependence for the behaviour of $\frac{\sigma_{L_3}}{\sigma_{L_2}}$ ratios at low projectile energy. In the theoretical work of Sarkadi and Mukoyama[8,9] it was shown that for heavy charged particle bombardment (Z>2) the experimental L_2 subshell ionization cross-section deviates by almost one order of magnitude from the RPWBA-BC theory. This anomalous behaviour was shown to be arising from collision induced transitions of a vacancy between the L-subshells. The large L_2 subshell ionization anomally was later theoritically accounted by Sarkadi and Mukoyama[10] by taking the subshell coupling effects into account.Recently Xu and Xu have made the calculation on L X-ray production cross sections of Bi for alpha particle bombardment using their own decay yield data[11] and ECPSSR ionization cross sections[12] and showed that their results are in good agreement with the experimental results[11] for the total X-ray production cross-section for alpha particle energy range (1.0-4.0)MeV.Looking at

the reported results of L-subshell ionnization of heavy elements one does not see a clear cut picture on the position of various ionization theories vis-a-vis the experimental results. The present study was aimed for obtaining various physical quantities such as X-ray production cross-sections.ionization cross-sections,relative L X-ray intensities and L-subshell ionization cross-section ratios etc from the measured data and compare with the existing theoritical calculations, so that one can get a clear cut picture on the process of L-subshell ionization by the bombardment of heavy charged particles.

II.Experimental Technique

The L X-ray spectra of Pb and Bi have been measured for alpha particle bombardment at different energies. High pure(~99.9%) samples were used for the preparation of the targets.Thin($40\mu g/cm^2$) targets of Pb and Bi were prepared by vaccum evaporation onto aluminized Mylar films of thickness $1.75mg/cm^2$.The targets were bombarded by alpha particles with energy 2.28 to 8.18MeV obtained from the 3MV tandem pelletron accelerator of the Institute. To obtain the L_i X-ray production cross-sections from the measured X-ray yields.simultaneous X-ray and elastically scattered charged particle detection technique was employed. Details of the experimental arrangement is described elsewhere[1]. The collimated alpha particle beamof 1.5mm diameter was directed onto the target which was kept tilted at 45° to the beam direction. The emitted L X-rays passed through a $3.5mg/cm^2$ mylar chamber-window, 5cm air gap and 0.012mm thick beryllium window before reaching the Si(Li) detector with energy resolution of 170eV(FWHM) at 5.9keV.The detector was placed at 90° to the beam direction.The solid angles of both the silicon surface barrier and Si(Li) detectors have been well defined by placing suitable aperatures in front of the detectors.Another adventage of the aperature was it allowed the radiation to fall on the center of the active area of the detector.A typical X-ray spectrum of Pb at 6MeV alpha particle energy is shown in Fig.1

III. Data analysis and Results

A. Data analysis

From the measured X-ray yields the L_i X-ray production cross-sections were estimated using the following relation:

$$\sigma^x_{L_i} = \frac{4\pi Y^i_x \sigma_R(\theta)\Delta\Omega_p}{\epsilon_a \epsilon_d Y_R \Delta\Omega_x}\left(\frac{t_x}{t_R}\right). \quad (1)$$

where,

$\sigma^x_{L_i}$ = X-ray production cross-section(the index i refers to a particular component of L X-ray such as l, α,β, γ etc.) of the L_i component of the L X-ray spectrum.

Y^i_x = Measured X-ray yield for the L_i component

$\sigma_R(\theta)$ = differential Rutherford scattering cross section

Y_R = Measured Rutherford yield

ϵ_d = Si(Li) detector intrinsic efficiency

ϵ_a = absorption correction for Mylar chamber window and air path

$\Delta\Omega_p$ = solid angle subtended by the charged particle silicon surface barrier detector.

$\Delta\Omega_x$ = solid angle subtended by the Si(Li) X-ray detector.

t_x = dead time correction for X-ray counting.

t_R = dead time correction for charged particle counting.

Intrinsic efficiency of the Si(Li) detector was theoritically calculated using the following expression:

$$\epsilon_d(E) = e^{-(\mu_{Be}x_{Be}+\mu_{Au}x_{Au}+\mu_{Si}\Delta x_{Si})}(1-e^{-\mu_{Si}x_{Si}}) \quad (2)$$

Where μ's are the absorption coefficients due to the Be window of the detector,the gold layer on the Si(Li) crystal and Si(Li) crystal at the X-ray energy E.Δx_{Si} is the thickness of the insensitive region of the Si(Li) crystal.The x's are as per specifications

of the detector manufacturer and the absorption coefficients are taken from the table of Hubbell et al[13].Y_x^i and Y_R^i are obtained from the measured X-ray and Rutherford spectra,respectvily. The X-ray yields for the various L X-ray components were estimated by the least square peak fitting programme and the Rutherford yields were calculated by summing the counts under the elastic peak.Corrections due to absorption in the Mylar chamber window and air-path were applied in the usual manner.Correction due to self absorption in the sample was found to be negligible.

In order to interpret the measured X-ray production cross-sections we tried to evaluate(1) the experimental subshell ionization cross-sections and their ratios and then compared with the theory and(2)compared the measured X-ray production cross-section ratios with the theoretical results obtained from theoretical ionization crosssections and the presently available different sets of decay yield data.For getting the experimental ionization cross-sections from the measured production cross-sections one runs through the following analytic formulas relating X-ray production cross-sections to the ionization cross-sections:

$$\sigma^x_{L_l} = (\sigma_{L_1} f_{13} + \sigma_{L_1} f_{12} f_{23} + \sigma_{L_2} f_{23} + \sigma_{L_3})\omega_3 F_{3l} \qquad (3a)$$

$$\sigma^x_{L_\alpha} = (\sigma_{L_1} f_{13} + \sigma_{L_1} f_{12} f_{23} + \sigma_{L_2} f_{23} + \sigma_{L_3})\omega_1 F_{1\alpha} \qquad (3b)$$

$$\sigma^x_{L_\beta} = \sigma_{L_1}\omega_1 F_{1\beta} + (\sigma_{L_1} f_{12} + \sigma_{L_2})\omega_2 F_{2\beta} + (\sigma_{L_1} f_{13} + \sigma_{L_1} f_{12} f_{23} + \sigma_{L_2} f_{23} + \sigma_{L_3})\omega_3 F_{3\beta} \qquad (3c)$$

$$\sigma^x_{L_\gamma} = \sigma_{L_1}\omega_1 F_{1\gamma} + (\sigma_{L_1} f_{12} + \sigma_{L_2})\omega_2 F_{2\gamma} \qquad (3d)$$

where $\sigma^x_{L_l}$,$\sigma^x_{L_\alpha}$,$\sigma^x_{L_\beta}$ and $\sigma^x_{L_\gamma}$ are the X-ray production cross-sections of the components of L_l,L_α,L_β and L_γ respectively.σ_{L_1}, σ_{L_2} and σ_{L_3} are ionization cross-sections of the subshells L_1,L_2 and L_3, respectively and ω_1,ω_2,and ω_3 are the corresponding subshell

fluoroscence yields.F_{ny} (F_{3l},$F_{3\alpha}$ ....etc) are the fraction of the radiative widths of the subshell L_n(L_1,L_2,L_3)contained in the yth spectral line i.e,

$$F_{ny} = \Gamma_{ny}/\Gamma_n \qquad (4)$$

(for example, $F_{3l} = \Gamma_{3l}/\Gamma_3$)where Γ_n is the total line width of L_n.The parameters f_{12},f_{23},and f_{13} are the Coster Kronig transition probabilities for $L_1 \rightarrow L_2$,$L_2 \rightarrow L_3$,and $L_1 \rightarrow L_3$ respectively(the arrow indicates the direction of the electron vacancy transition between subshells).

The composite L_γ peak has been computer analysed into four Gaussians whose χ^2 value was found to be close to one for all projectile energies. Four components of L_γ were obtained ; L_{γ_5} and L_{γ_1} which are related to the L_2 subshell and $L_{\gamma_{2+3}}$ and L_{γ_4} which are related to L_1 subshell.Examples of this fitting for Pb and Bi at one projectile energy are presented in Fig.2. Equation(3d) can be broken into.

$$\sigma^x_{L_{\gamma_{2+3}}} + \sigma^x_{L_{\gamma_4}} = \sigma_{L_1}\omega_1 F_{1\gamma_{2+3+4}} \qquad (5)$$

and,

$$\sigma^x_{L_{\gamma_5}} + \sigma^x_{L_{\gamma_1}} = (\sigma_{L_1} f_{12} + \sigma_{L_2})\omega_2 F_{2\gamma_{5+1}} \qquad (6)$$

Equations (5) and (6) can be solved iteratively for σ_{L_1} and σ_{L_2} by first ignoring f_{12} in equations(6) and (3d). σ_{L_3} was obtained through equation(3b) by using the deduced σ_{L_1} and σ_{L_2} and the measured X-ray production cross-section $\sigma^x_{L_\alpha}$.After this a consistence check was made for the L_β group through the comparison between the measured $\sigma^x_{L_\beta}$ and that calculated from equation(3c). The average difference between the calculated and measured $\sigma^x_{L_\beta}$ was found to be (3.0-4.0)% for the entire energy range.

B.Atomic Parameters

The measured X-ray production cross sections are converted into ionization cross sections by using two sets of fluoroscence yield data ,one by Krause[14] and the other by Xu and Xu[11]. The fractional widths used here are taken from the radiative emmision rates calculated by Scofield[15].The atomic parameters used in the present work are given in table-1.

C.Results and Error analysis

The ionization cross sections σ_{L_1},σ_{L_2} and σ_{L_3} for Pb and Bi ,obtained as described before,are shown in Figs. 3 & 4. together with the two theoretical results which will be discussed below.

The standard counting error for the L_α X-rays was 0.5%.L_β X-rays 0.7% and L_γ X-rays which relate to L_1 and L_2 subshell ionization was on the average less than 5%. In addition to this the other sources of experimental uncertainty come from the detector efficieny and absorption correction due to Mylar chamber window and airpath.They contribute together an overall error of about 2.0% . The self absorption in the target was negligible.Uncertainty in the estimation of the solid angles will be within 5.0% .

In the conversion process to ionization cross sections from X-ray yields,uncertainties in the atomic parameters,such as fluoroscence yield ,radiative transition rates and Coster-Kronig transition probabilities may increase the uncertainty for the final absolute ionization cross sections.The error from this source could amount to about 10% .The error in the ratio of ionization cross sections $\frac{\sigma_{L_1}}{\sigma_{L_2}}$, $\frac{\sigma_{L_3}}{\sigma_{L_2}}$ will be mainly from the counting error.

IV.Discussion

The absolute ionization cross sections of Pb & Bi which are plotted in Figs. 3 & 4 show deviations in opposite directions from the ECPSSR theory[12] for σ_{L_1} & σ_{L_2}.However the ionization cross sections for L_3 and total(see table-2) are in good agreement(within 6.0% on average)with the theory[12].In a previous work by Chang et al[4] the ionization cross section for L_2 subshell ionization for alpha particle bombardment was shown to be in good agreement with PWBA theory[7] but our present study shows large deviations in the entire projectile energy range.However,the discrepancies found in our present results for σ_{L_1} and σ_{L_2} are consistent with the heavy ion data of Sarkadi and Mukoyama[8].In Figs. 3 & 4 we have shown two sets of measured ionization cross sections corresponding to two different sets of decay yield data by Krause[14] and Xu & Xu[11].As can be seen from the figures the decay yield data of Krause[14] gives better agreement with theory for L_1 and L_3 subshell ionization cross sections whereas the decay yield data of Xu & Xu[11] gives better agreement with theory for σ_{L_2}. Further comparison with theory is done by plotting the ionization cross section ratios $\frac{\sigma_{L_1}}{\sigma_{L_2}}$ and $\frac{\sigma_{L_3}}{\sigma_{L_2}}$ in Figs. 5 & 6.The measured ratios show large deviations from the ECPSSR theory,especially at low projectile energy the discrepancy is quite large.For both Pb and Bi the measured ratio $\frac{\sigma_{L_1}}{\sigma_{L_2}}$ is found to be lower compared to the theoritical value and position of the dip of the experimental curve is shifted to the left of the theoritical dip.Such a shift was also seen in the previous works[4,5].In Fig.5b we have also plotted the result of RPWBA-DHS-BC calculation[6] for proton ionization which seems to be in better agreement with the experimental result.The RPWBA-DHS-BC theory also produces the dip at the right place.This suggests that the target electron wave functions play an important role for predicting the dip of the $\frac{\sigma_{L_1}}{\sigma_{L_2}}$ curve correctly.The theoritical results for the $\frac{\sigma_{L_3}}{\sigma_{L_2}}$ ratios(Fig. 6) of both Pb and Bi again show large discrepancies from the experimental results.Previous measurements[3-5] showed a drop in the $\frac{\sigma_{L_3}}{\sigma_{L_2}}$ ratio at low projectile enegy (below 1MeV/amu), but in our

present study we do not see a clear cut drop in the value of the ratio.At the same time we also do not see any rising trend as predicted by theory and as observed in the case of ionization by protons.Our present result of $\frac{\sigma_{L_3}}{\sigma_{L_2}}$ ratios are more closer to the results of Chang et al[3],who also did not see any drop for the elements with closed 6s configuration.Both Pb and Bi have closed 6s configuration.The kind of drop seen by Li et al[5] for all elements irrespective of the outer electronic configuration of the target atom has not been confirmed by our present results.In Fig.6b we have also plotted the theoritical $\frac{\sigma_{L_3}}{\sigma_{L_2}}$ ratio for proton ionization obtained from the RPWBA-DHS-BC theory[6] which shows better agreement with the experimental ratio. This again suggests that the target electron wavefunctions play an important role in the calculation of ionization cross sections.

The measured X-ray production cross section ratios of Pb and Bi are compared with the theoretical results in Figs. 7 & 8 .Although the theoretical results calculated using the decay yield data of Xu and Xu[11] agree better with the experimental results,one should not take this agreement very seriously because it may so happen that the absolute X-ray production cross sections(Figs.9 & 10) are not in good agreement but their ratio is good.Evidence in favour of this argument can be seen in the comparison of absolute ionization cross sections shown in Figs.3 & 4.

The experimental centroid energies of the composite L X-ray peaks are estimated as given in the reference of Bissinger et al[17] and compared with the theoretical calculations in Figs. 11 & 12. Since the L_α transition involves only the L_3 subshell no shift of the centroid energy is expected for this line with projectile energy unless there is any multi-vacancy formation and none is observed.Relative variation in L-subshell hole production is expected to produce a beam energy dependent shift in the centroid positions of L_β and L_γ lines which are composite lines with contribution from at least two subshells. Variation of L_β centroid energy with α-particle energy is well explained by the ECPSSR

theory[12] for both Pb and Bi. However, in the case of L_γ centroid energy we find some discrepancy between theory and experiment.Moreover the discripancy in the case of Pb is at the low projectile energy and for Bi it is at high energy side. The reason for this difference is not quite clear to us .It may be because of the fact that the hole-subshell cross section ratio variation with bombarding energy predicted by the theory is not correct for different parts of the projectile energy range in Pb and Bi.

In summary,we would like to say that the present study on L-subshell ionization in Pb and Bi by α particles has revealed some new features of the ionization process.The ECPSSR theory is found to be inadequate in explaining the measured L_1 and L_2 subshell ionization cross sections. Calculations taking into account the collision induced intrashell transition effects are needed in order to remove the present discrepancy between theory and experiment.

We also feel that the problem of dependence of α-particle induced L shell ionization on outer electron configuration of the target atom is not yet fully setteled.Although the work of Li et al[5] has ruled out this dependence,our present study keeps the problem alive again and it is necessary to carry out a systematic study on many targets with filled and unfilled 6s state inorder to get a clearer picture on the problem. In order to check this point our next plan will be to carry out fresh measurements in some more elements with the atomic number in the region 70<Z<94.

References:

1. H.C.Padhi,C.R.Bhuinya,B.B.Dhal and S.Mishra,J.Phys B: At.Mol.Opt.Physics(Communicated).
2. S.Datz,J.L.Duggan,L.C.Feldman,E.Laegsgaard,and J.U.Anderson, Phys. Rev. A9 192,(1974)
3. C.N.Chang,J.F.Morgan and S.L.Blatt,Phys.Letters 49A, 365(1974)
4. C.N.Chang,J.F.Morgan and S.L.Blatt,Phys.Rev. A11,607(1975)
5. T.K.Li,D.L.Clark and G.W.Greenlees,Phys.Rev.Letters. 37, 1209(1976).
6. J.Braziewicz.E.Braziewicz.J.Ploskonika.M.Pajek and G.M.Osetynski.J.Phys.B At.Mol.Phys. 17,3245(1984).
7. B.H.Choi.E.Merzbacher and G.S.Khandelwal.At.Data 5,291(1973).
8. L.Sarkadi and T.Mukoyama.J.Phys.B13,2255(1980).
9. L.Sarkadi and T.Mukoyama.J.Phys.B14,L255(1981).
10. L.Sarkadi and T.Mukoyama.Phys.Rev.A37,4540(1988)
11. J.Q.Xu and X.J.Xu J.Phys.B At.Mol.Opt.Phys.25,695(1992) and references therein.
12. D.D.Cohen and M.Harrigan.Atomic Data Nuclear Data Tables 33,255(1985)
13. J.H.Hubbell.W.H.McMaster.N.K.Del Grande and J.H.Hammellet in J.A.Ibers and J.C.Hamilton(ed.) International Tables for X-ray crystallography vol.4 (Keynoch press.Birmingham).47(1974)
14. M.O.Krause.J.Phys.Chem.Ref.Data 8,307(1979).
15. J.H.Scofield.Phys.Rev.A10,1507(1974)
16. M.H.Chen and B.Crasemann Atomic Data Nuclear Data Tables33,217(1985);41,257(1989).
17. G.A.Bissinger.A.B.Baskin.B.H.Choi.S.M.Safroth.J.M.Howard and A.W.Waltner.Phys.Rev.A6,545(1972).

Figure Captions:

Fig.1 A typical L X-ray spectrum of Pb at a α-particle energy of 6MeV.

Fig.2 Gaussian fits to the L_γ X-ray spectra of (a)Pb and (b)Bi.The χ^2 values of the fits are indicated.

Fig.3 L-shell ionization cross-sections of Pb for α-particle bombardment .(a) L_1 subshell,(b) L_2 subshell,(c)L_3 subshell: (....)corresponds to ECPSSR theory ;(—)corresponds to present experimental results obtained from the data using the decay yield data of Xu and Xu ;(- - -) corresponds to present experimental results obtained the data using the decay yield data of Krause.

Fig.4 L-shell ionization cross sections of Bi (a)L_1 subshell, (b)L_2 subshell, (c)L_3 subshell: (....) corresponds to ECPSSR theory ;(—) corresponds to present experimental results obtained from the data using the decay yield data of Xu and Xu ;(- - -) corresponds to present experimental results obtained from the data using the decay yield data of Krause.

Fig.5 Values of the ionization cross section ratio $\frac{\sigma_{L_1}}{\sigma_{L_2}}$ of (a)Pb and (b)Bi:(- - -) corresponds to ECPSSR theory.(....) corresponds to RPWBA-DHS-BC theory ;solid line joining the experimental points(•) is obtained using Krause's decay yield data ;solid line joining the experimental points(o) is obtained using Xu and Xu's decay yield data.

Fig.6 Values of ionization cross-section ratio $\frac{\sigma_{L_3}}{\sigma_{L_2}}$ of (a) Pb and (b) Bi:(- - -) corresponds to ECPSSR theory.(.....) corresponds to RPWBA-DHS-BC theory ;solid line joining the experimental points(•) is obtained using the decay yield data of Krause ;solid line joining the experimental points(o) is obtained using the decay yield data of Xu and Xu.

Fig.7 Various ratios of X-ray production cross sections of Pb for α-particle bombardment (a)$\frac{\sigma_\gamma^2}{\sigma_\gamma^2}$, (b)$\frac{\sigma_\gamma^2}{\sigma_\gamma^2}$ and (c)$\frac{\sigma_\gamma^2}{\sigma_\gamma^2}$.The solid line corresponds to the eye fitted line drawn through the experimental points ;(...) corresponds to result obtained by using the ECPSSR ionization cross-sections and decay yield data of Xu and Xu ,(- - -) cor-

responds to results obtained by using ECPSSR ionization cross-sections and decay yield data of Krause.

Fig.8 Various ratios of X-ray production cross-sections of Bi for α-particle bombardment (a)$\frac{\sigma_\alpha^x}{\sigma_\gamma^x}$,(b)$\frac{\sigma_\alpha^x}{\sigma_\beta^x}$ & (c)$\frac{\sigma_\alpha^x}{\sigma_\gamma^x}$ .The solid line corresponds to eye fitted line drawn through the experimental points ; (....) corresponds to results obtained by using ECPSSR ionization cross-sections and decay yield data of Xu and Xu ;(- - -)corresponds to the results obtained by using ECPSSR ionization cross sections and decay yield data of Krause.

Fig.9 Total X-ray production cross sections of Pb for α-particle bombardment in the energy range (0.57-2.2)MeV/amu;(•) present experimental data ;(——) corresponds to result obtained from ECPSSR ionization cross-sections and decay yield data of Krause ;(- - -) corresponds to results obtained from ECPSSR ionization cross sections and decay yield data of Xu and Xu.

Fig.10 Total X-ray production cross section of Bi for α-particle bombardment in the energy range (0.57- 2.2)MeV/amu,(•) corresponds to present experimental points ;(——) corresponds to results obtained from ECPSSR ionization cross section and decay yield data of Krause ;(- - -)corresponds to results obtained from ECPSSR ionization cross sections and decay yield data of Xu and Xu.

Fig.11 Centroid energies of various L X-ray lines of Pb.The solid lines are the eye fitted lines drawn through the experimental points(•) ;(....) orresponds to results obtained from ECPSSR theory and decay yield data of Xu and Xu : (- - -) corresponds to results obtained from ECPSSR theory and decay yield data of Krause.

Fig.12 Centroid energies of various L X-ray lines of Bi.The solid lines are the eye fitted lines drawn through the experimental points(•) ;(....)corresponds to results obtained from ECPSSR theory and decay yield data of Xu and Xu ;(- - -) corresponds to results obtained from ECPSSR theory and decay yield data of Krause.

Table 1: L-subshell Fluoroscence and Coster-Kronig yields of Pb & Bi

Target Atom	Decay yield data set	ω_1	ω_2	ω_3	f_{12}	f_{13}	f_{23}
Pb	Krause[14]	0.112	0.373	0.360	0.12	0.58	0.116
	Xu & Xu[11]	0.135	0.405	0.326	0.040	0.661	0.091
Bi	Krause[14]	0.117	0.387	0.373	0.11	0.58	0.113
	Xu & Xu[11]	0.138	0.428	0.340	0.055	0.700	0.12

Table 2: Total L-shell ionization cross-section of Pb & Bi for α-particle bombardment

α-particle energy	σ_{L_T} of Pb (barn)			σ_{L_T} of Bi (barn)		
	Theory	Expt. using decay yields		Theory	Expt. using decay yields	
MeV/amu	ECPSSR	Krause	Xu& Xu	ECPSSR	Krause	Xu& Xu
0.571	7.291	7.220	7.419	6.252	6.603	6.368
0.757	18.566	19.518	20.102	16.104	15.091	14.463
0.937	35.301	39.921	41.219	30.805	30.664	29.228
1.224	58.743	64.557	66.703	51.484	53.014	50.530
1.306	87.276	96.499	99.751	76.715	73.237	69.698
1.492	122.355	135.086	139.570	107.766	111.250	108.390
1.675	162.463	179.266	185.194	143.313	158.727	150.905
1.863	209.117	229.915	237.279	184.823	203.302	193.460
2.046	260.752	286.482	295.527	229.572	254.820	243.019

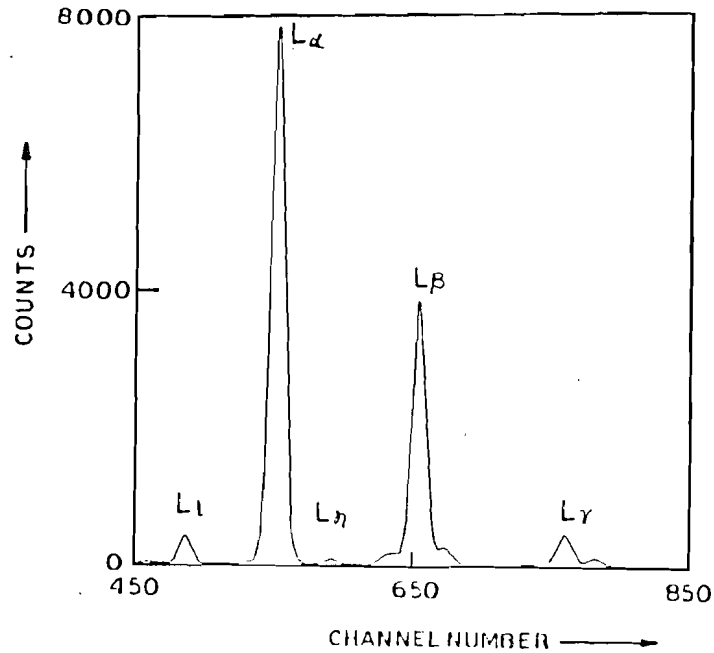
8000
4000
0
COUNTS
Lα
Lβ
Ll
Lη
Lγ
450
650
850
CHANNEL NUMBER

Fig. 1

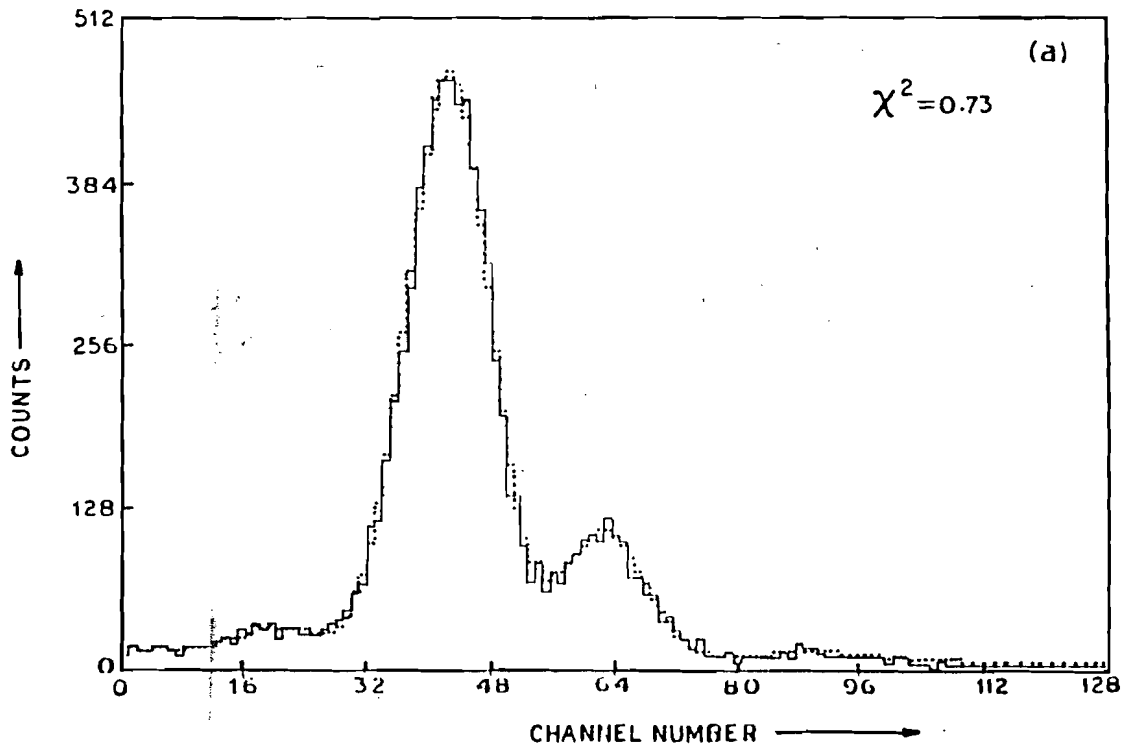
512
384
256
128
0
COUNTS
(a)
$\chi^2 = 0.73$
0
16
32
48
64
80
96
112
128
CHANNEL NUMBER

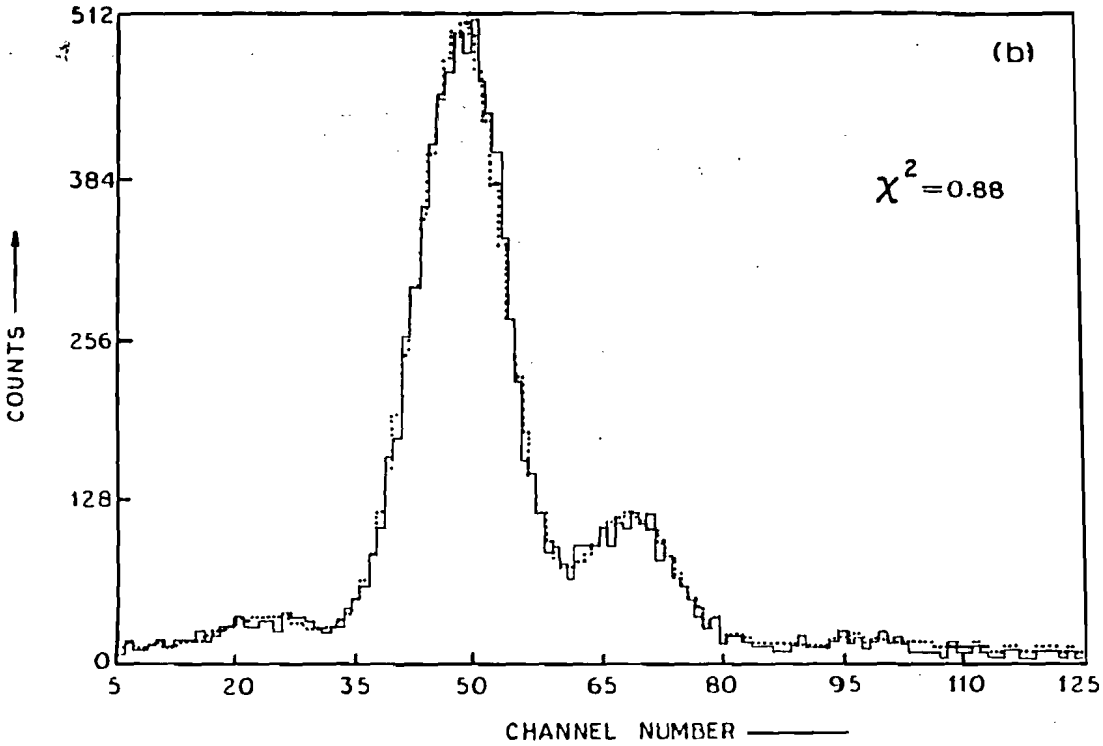
(b)
χ^2=0.88
COUNTS
512
384
256
128
0
5
20
35
50
65
80
95
110
125
CHANNEL NUMBER

Fig. 2b

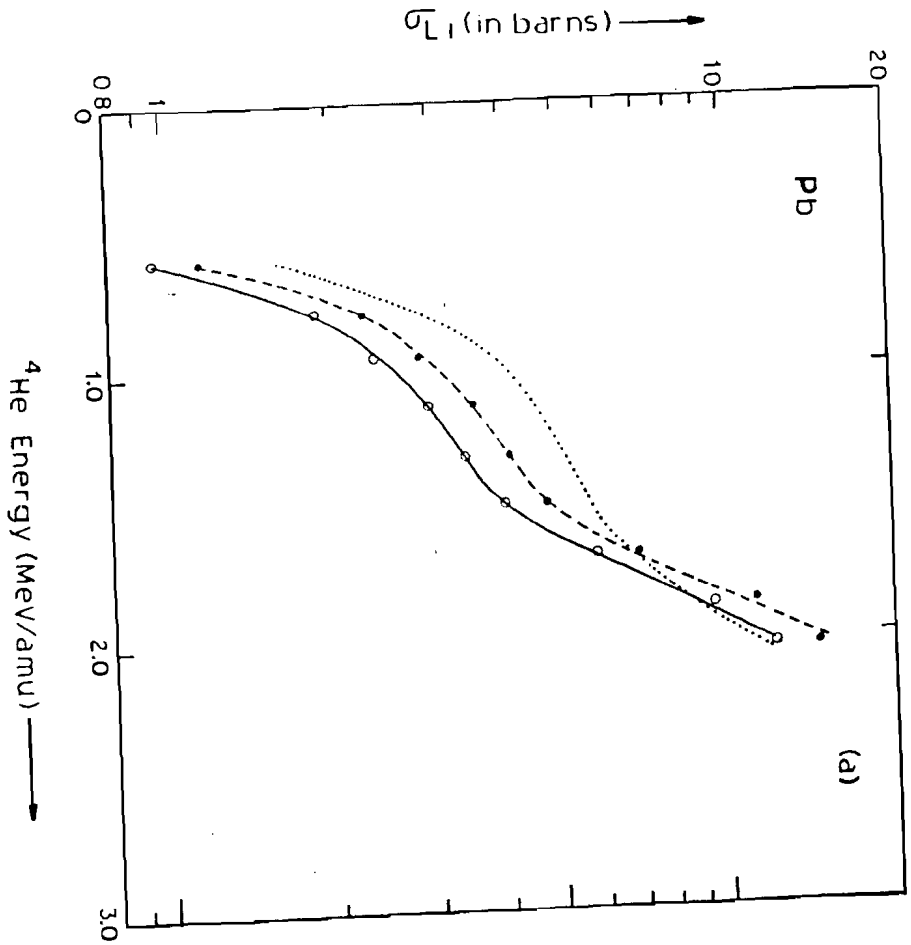
(a)
Pb
σ_{L_1} (in barns)
20
10
1
0.8
0
1.0
2.0
3.0
^{4}He Energy (MeV/amu)

Fig. 3a

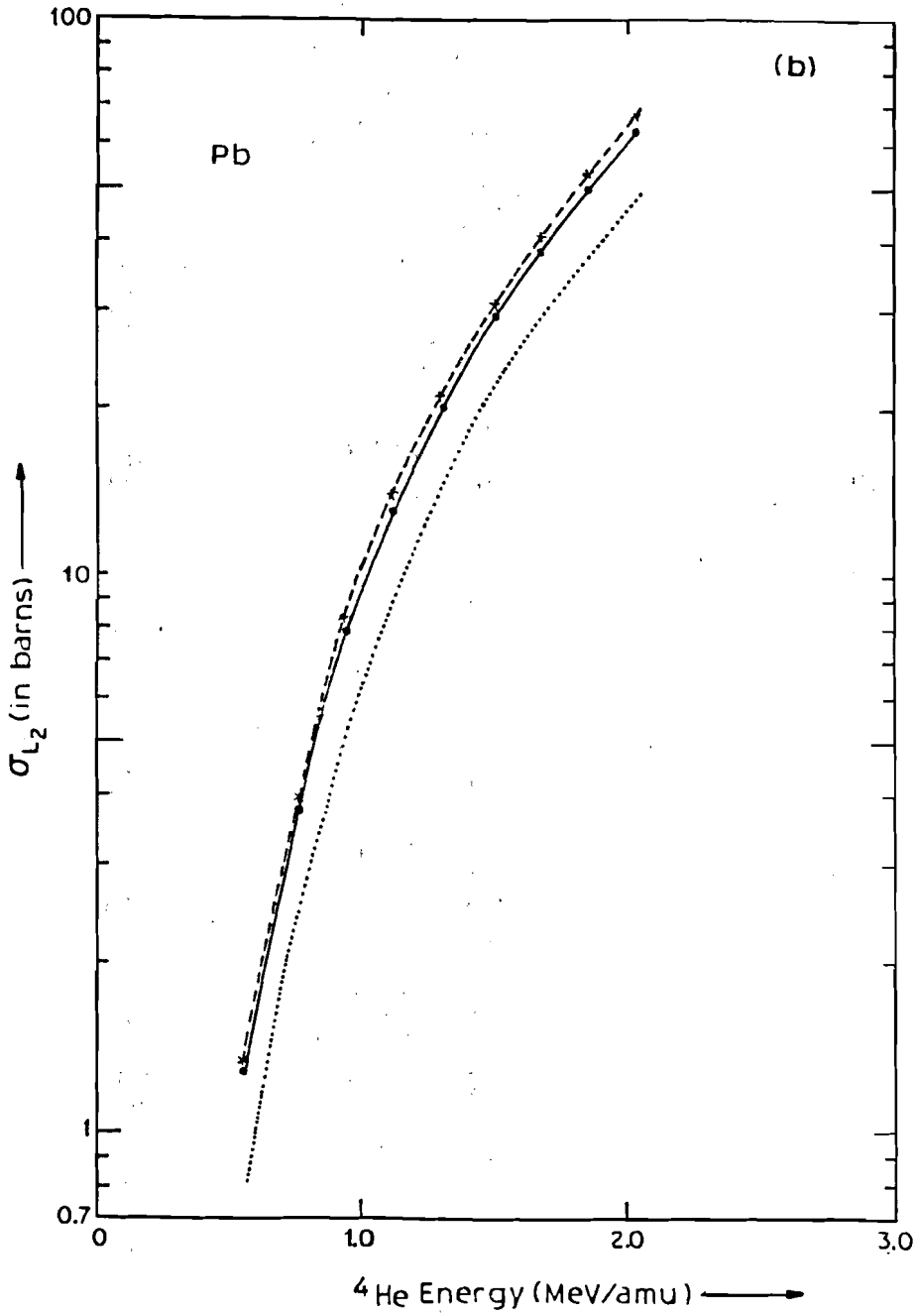
(b)
Pb
100
10
1
0.7
0
1.0
2.0
3.0
σ_{L_2} (in barns)
^{4}He Energy (MeV/amu)

Fig.3b

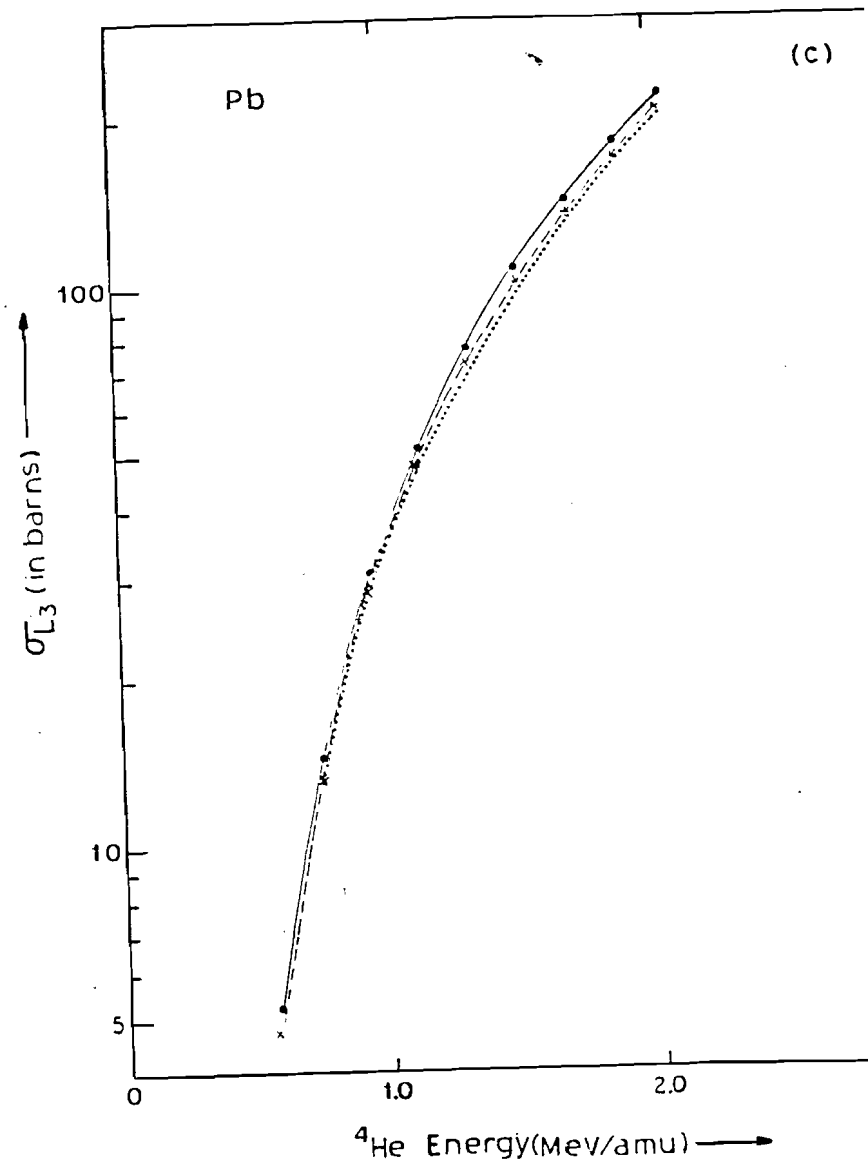
(c)
Pb
100
10
5
0
1.0
2.0
σ_{L_3} (in barns)
^{4}He Energy(MeV/amu)

Fig.3c

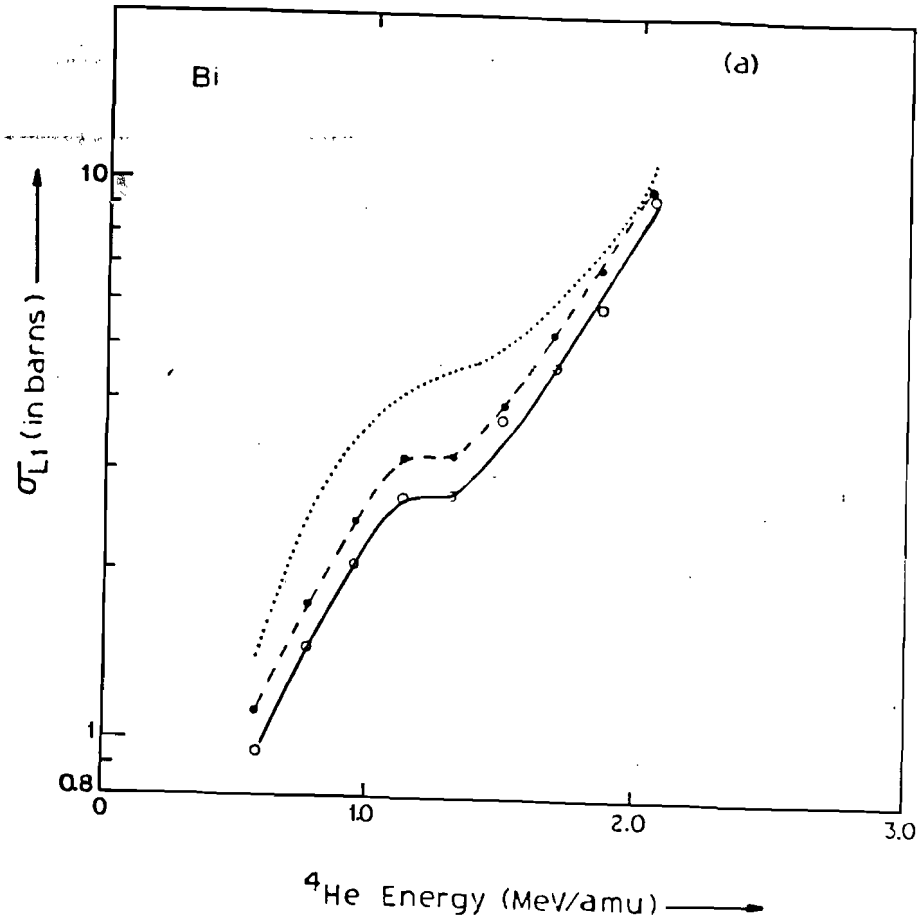
Bi
(a)
10
1
0.8
0
1.0
2.0
3.0
σ_{L1} (in barns)
^{4}He Energy (MeV/amu)

Fig. 4a

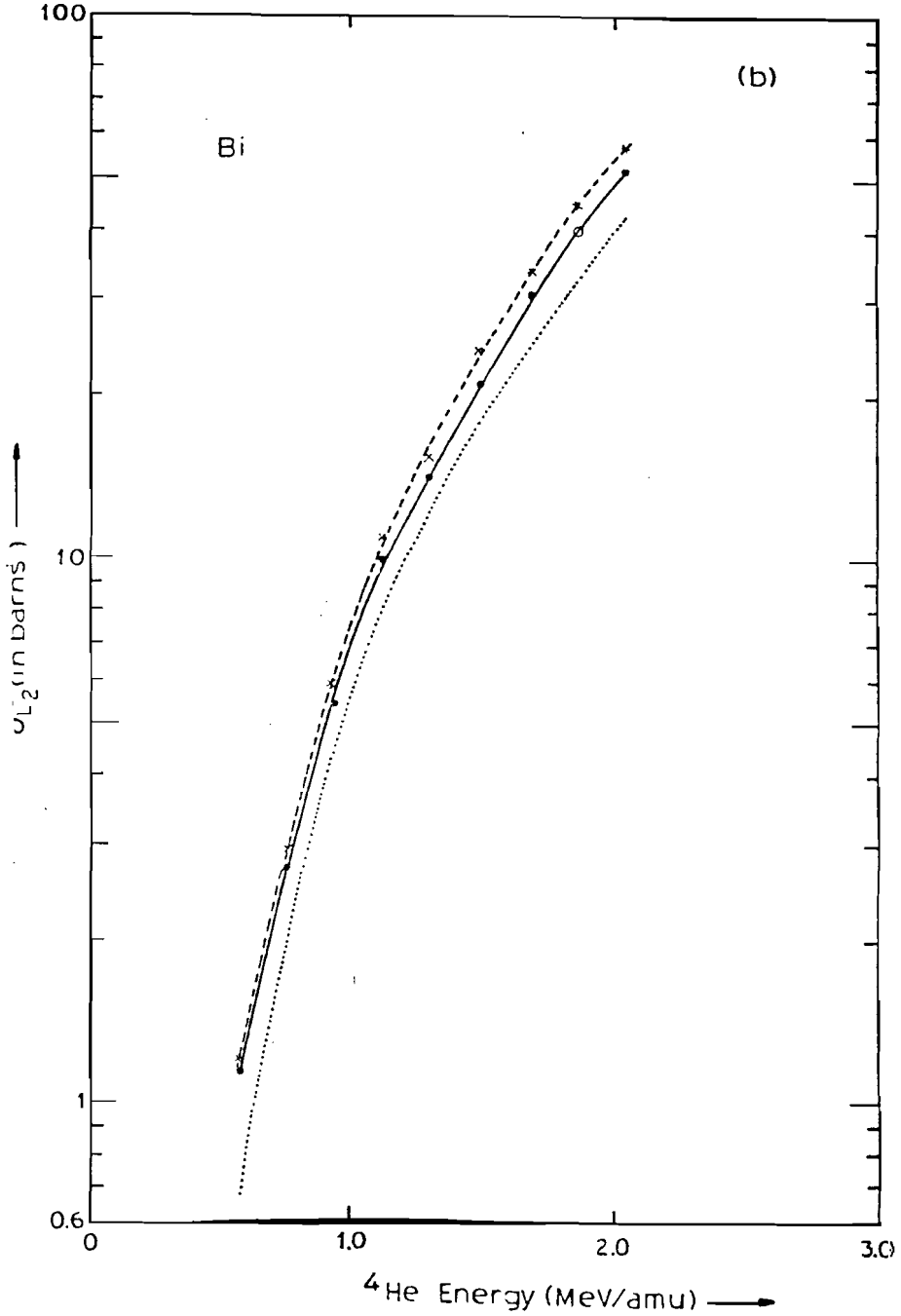
100
(b)
Bi
10
1
0.6
0
1.0
2.0
3.0
σ_{L2} (in barns)
^{4}He Energy (MeV/amu)

Fig. 4b

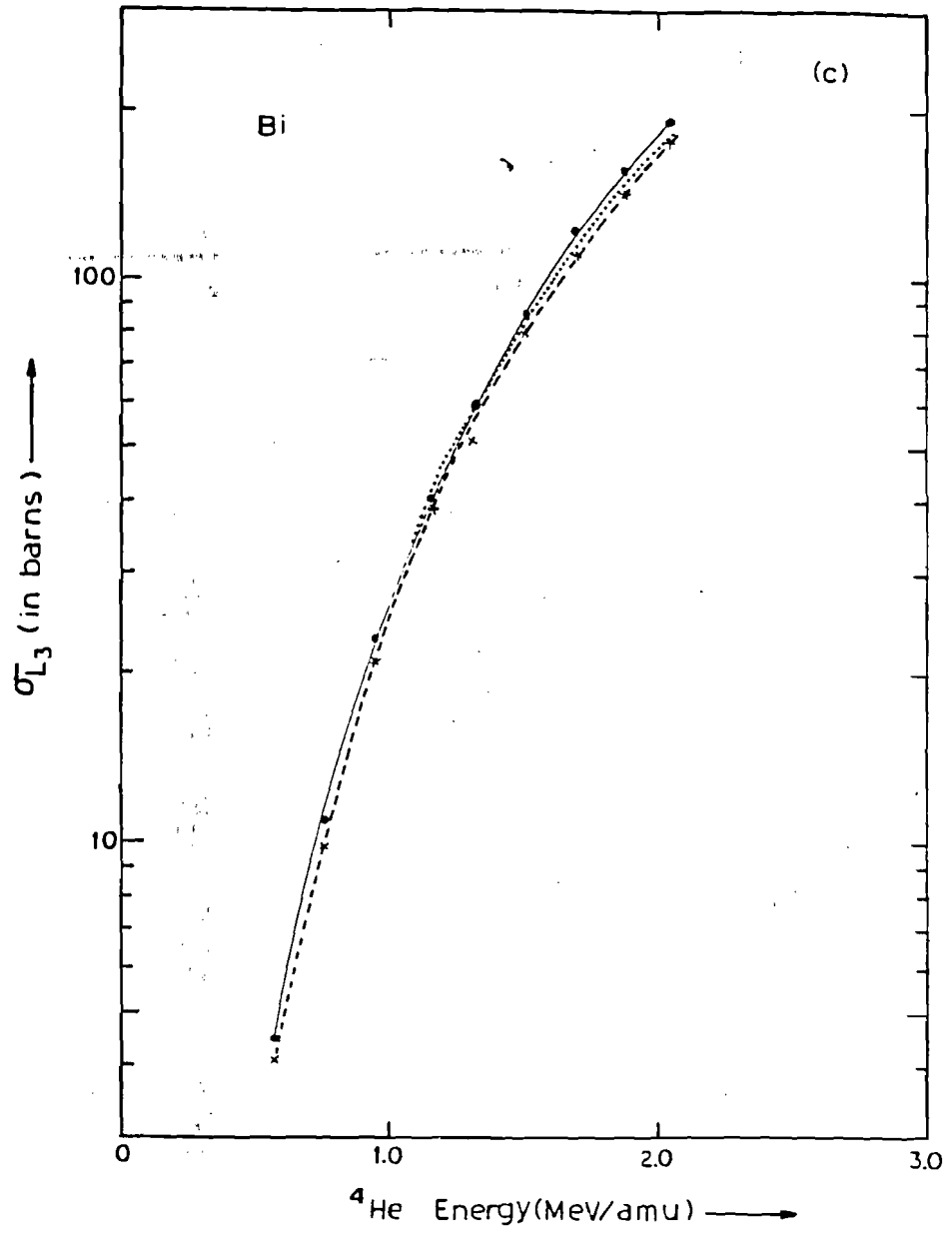
(c)
Bi
100
10
0
1.0
2.0
3.0
σ_{L_3} (in barns)
^{4}He Energy(MeV/amu)

Fig-4c

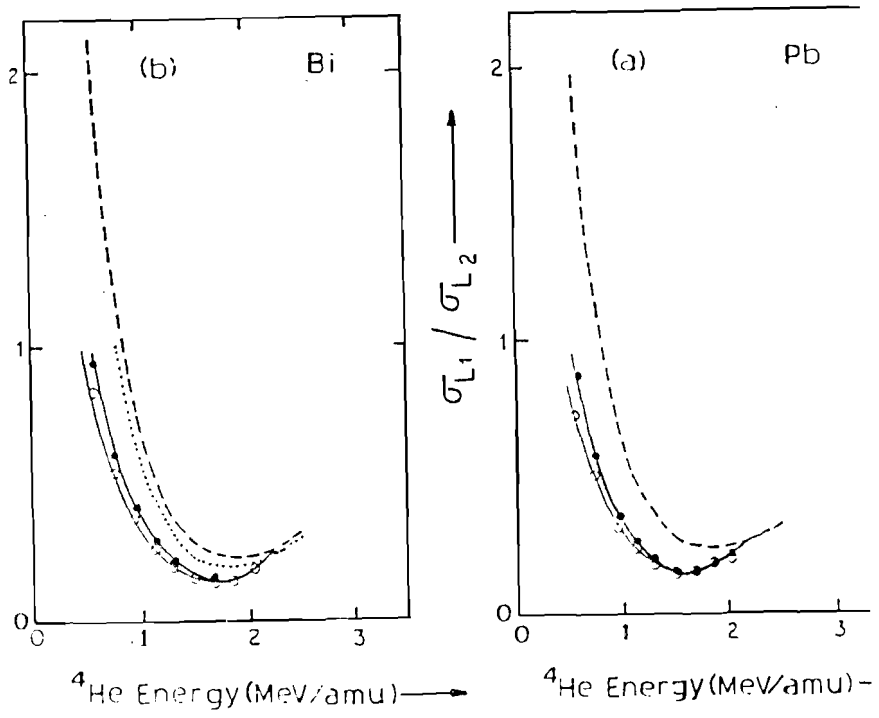
(b)
Bi
(a)
Pb
2
1
0
0
1
2
3
$\sigma_{L_1} / \sigma_{L_2}$
^{4}He Energy(MeV/amu)
^{4}He Energy(MeV/amu)

Fig-5

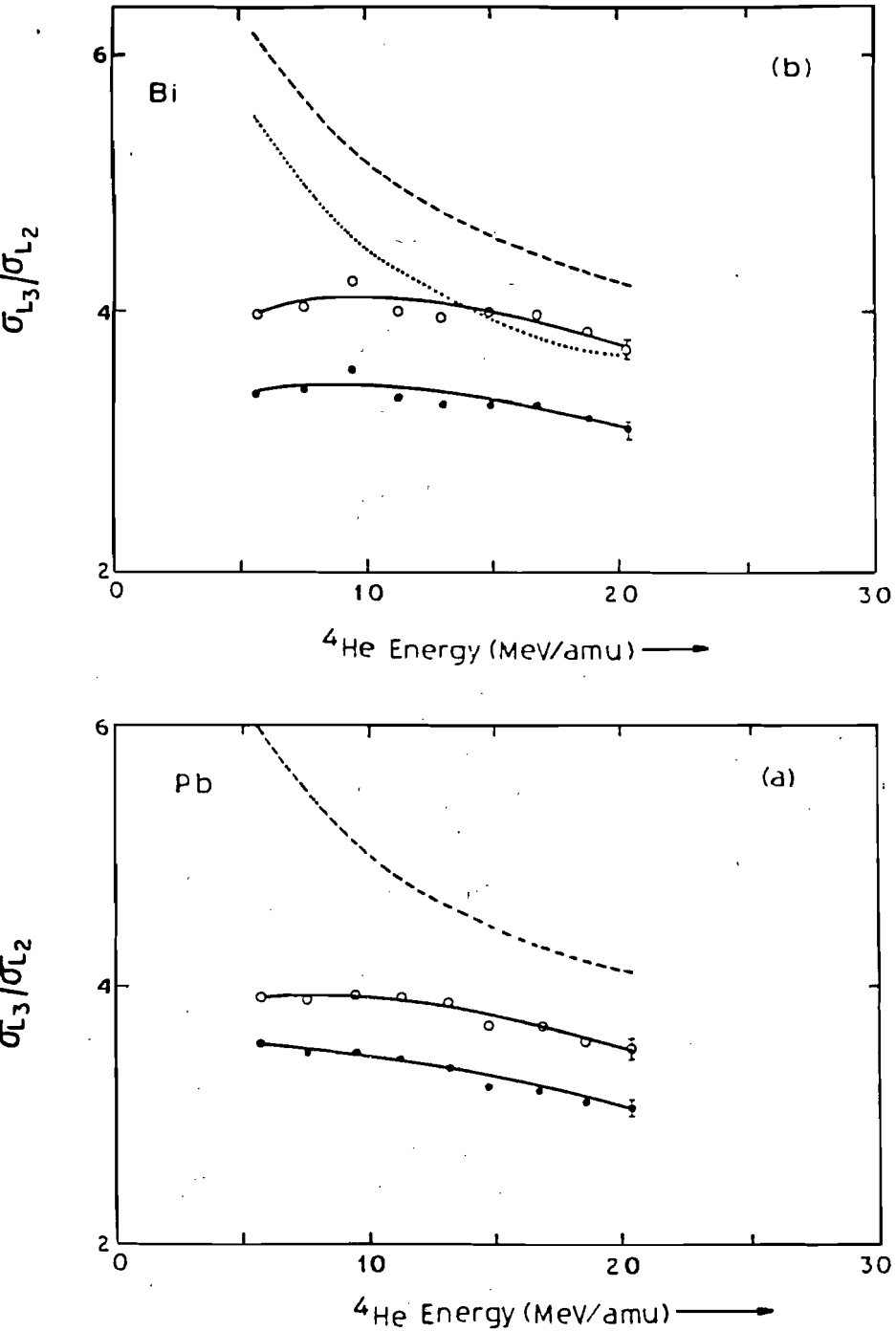
Bi
(b)
Pb
(a)
$\sigma_{L_3}/\sigma_{L_2}$
^{4}He Energy (MeV/amu)

Fig. 6

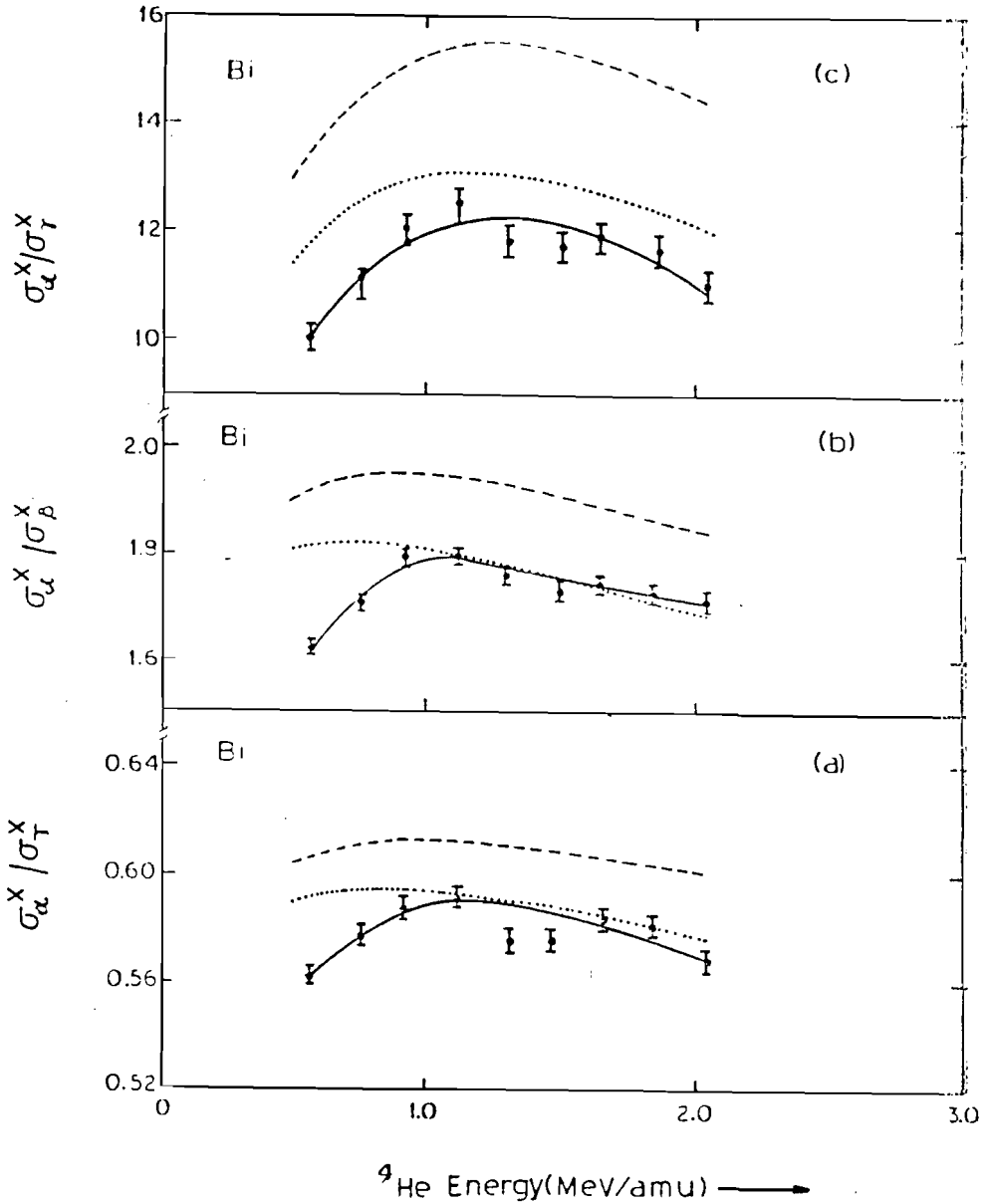
Bi
(c)
(b)
(a)
$\sigma_\alpha^x/\sigma_T^x$
^{4}He Energy(MeV/amu)

Fig. 7

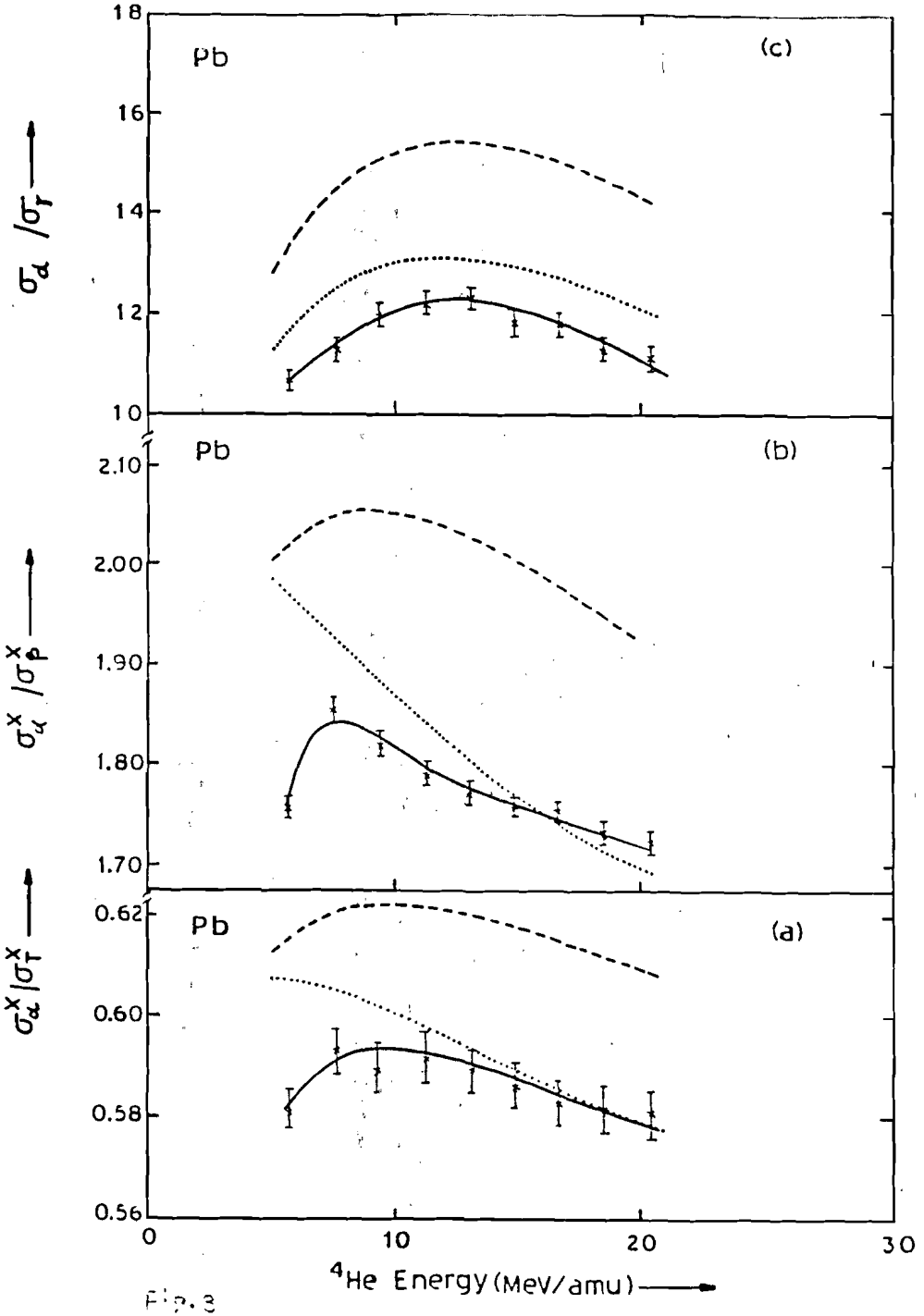
Pb
(c)
Pb
(b)
Pb
(a)
σ_α / σ_T
$\sigma_\alpha^x / \sigma_p^x$
$\sigma_\alpha^x / \sigma_T^x$
^{4}He Energy (MeV/amu)

Fig. 3

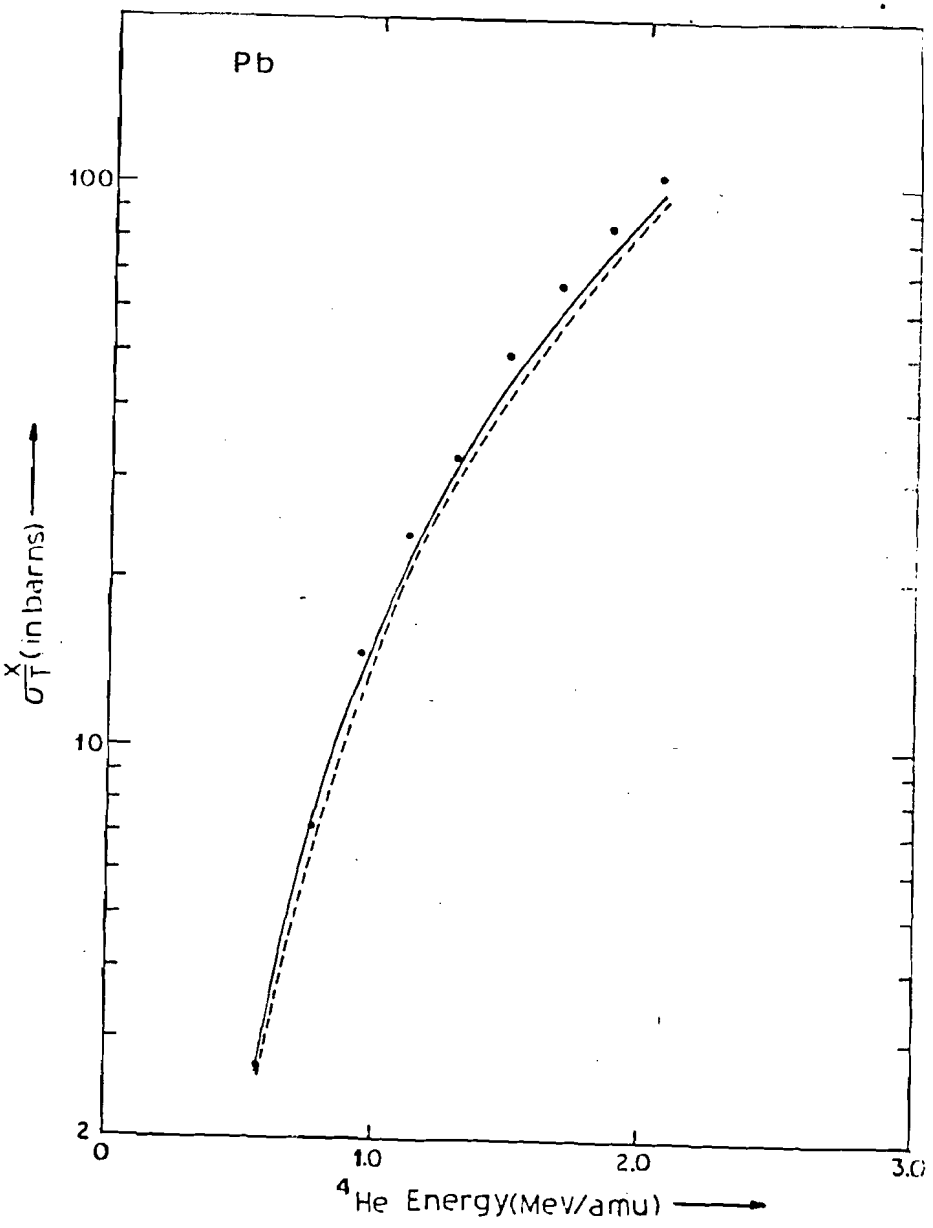
Pb
σ_T^x (in barns)
^{4}He Energy(MeV/amu)

Fig. 9

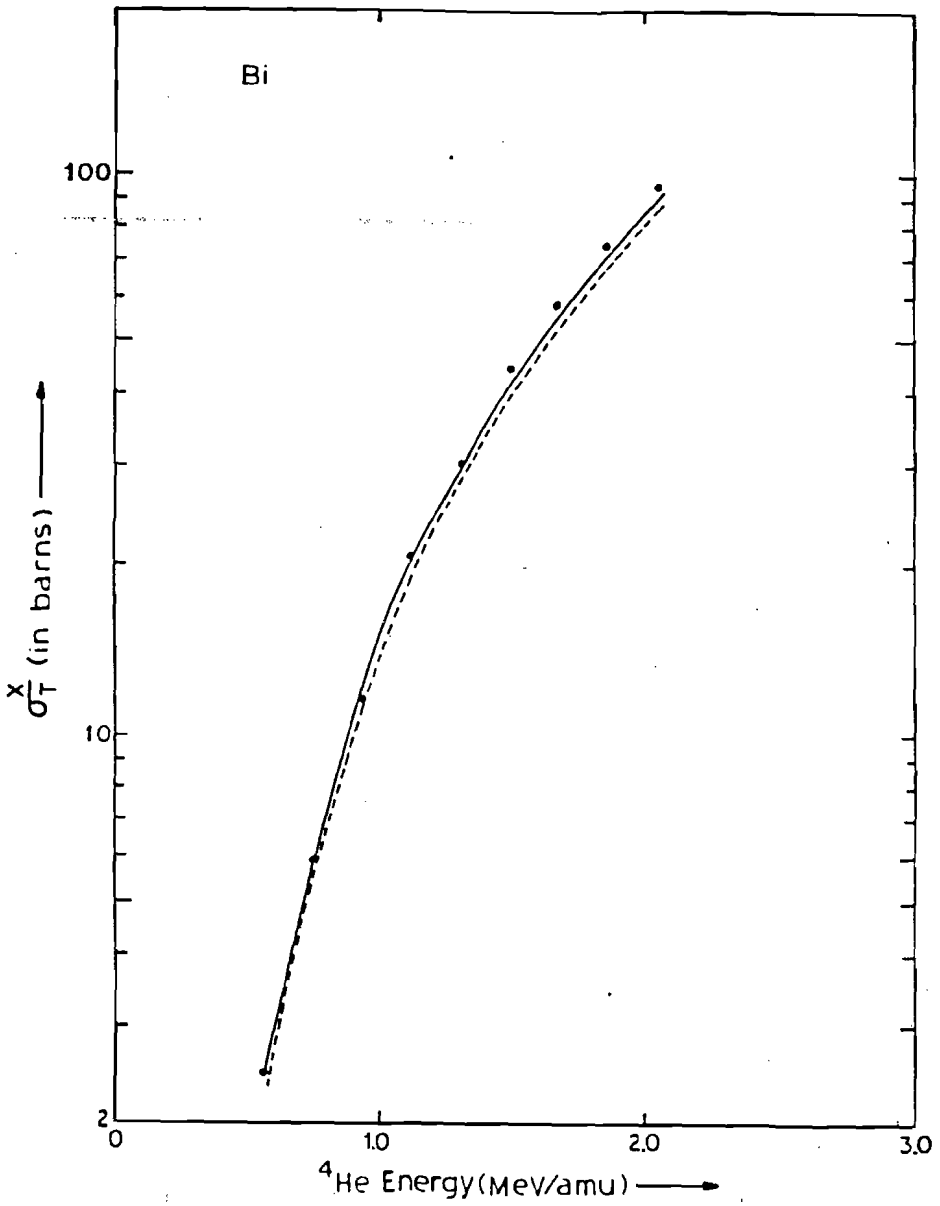
Bi
100
10
2
0
1.0
2.0
3.0
σ_T^x (in barns)
^{4}He Energy(MeV/amu)

Fig. 10

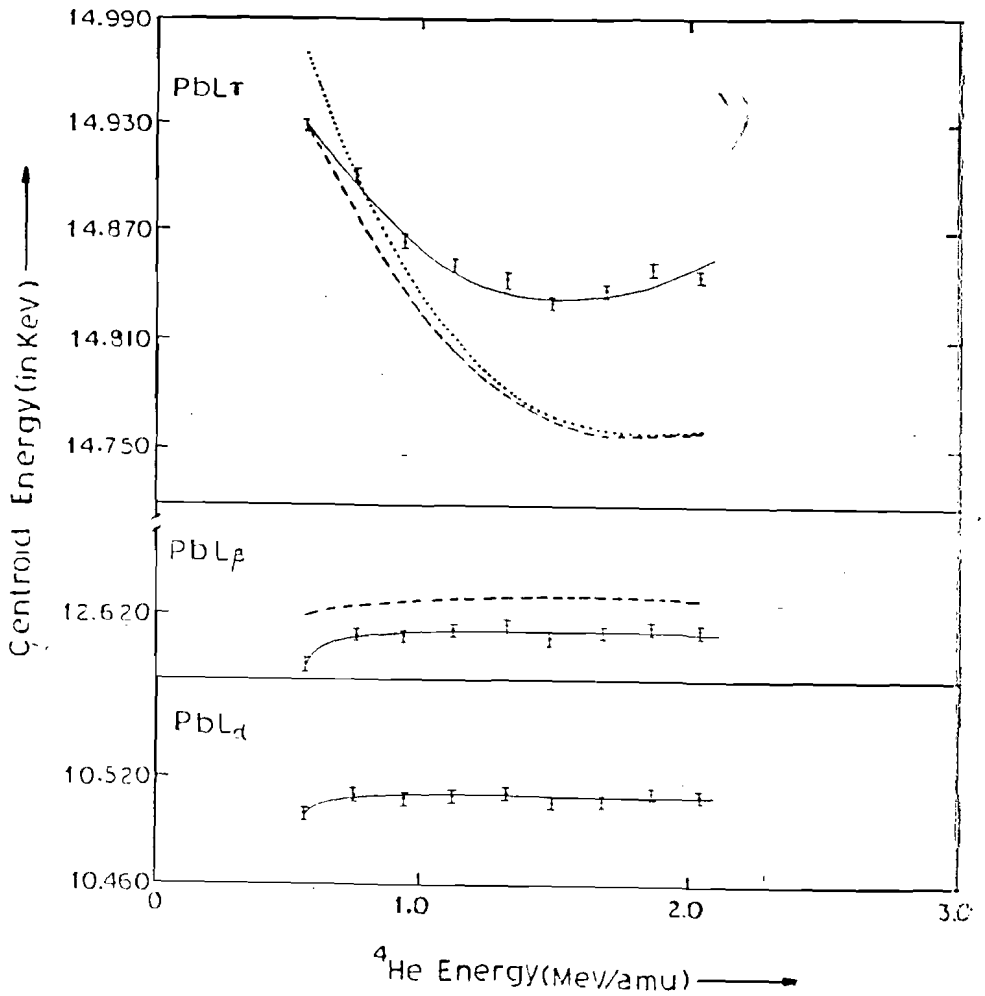
14.990
14.930
14.870
14.810
14.750
PbLτ
PbLβ
12.620
PbLα
10.520
10.460
0
1.0
2.0
3.0
Centroid Energy(in Kev)
^{4}He Energy(Mev/amu)

Fig. 11

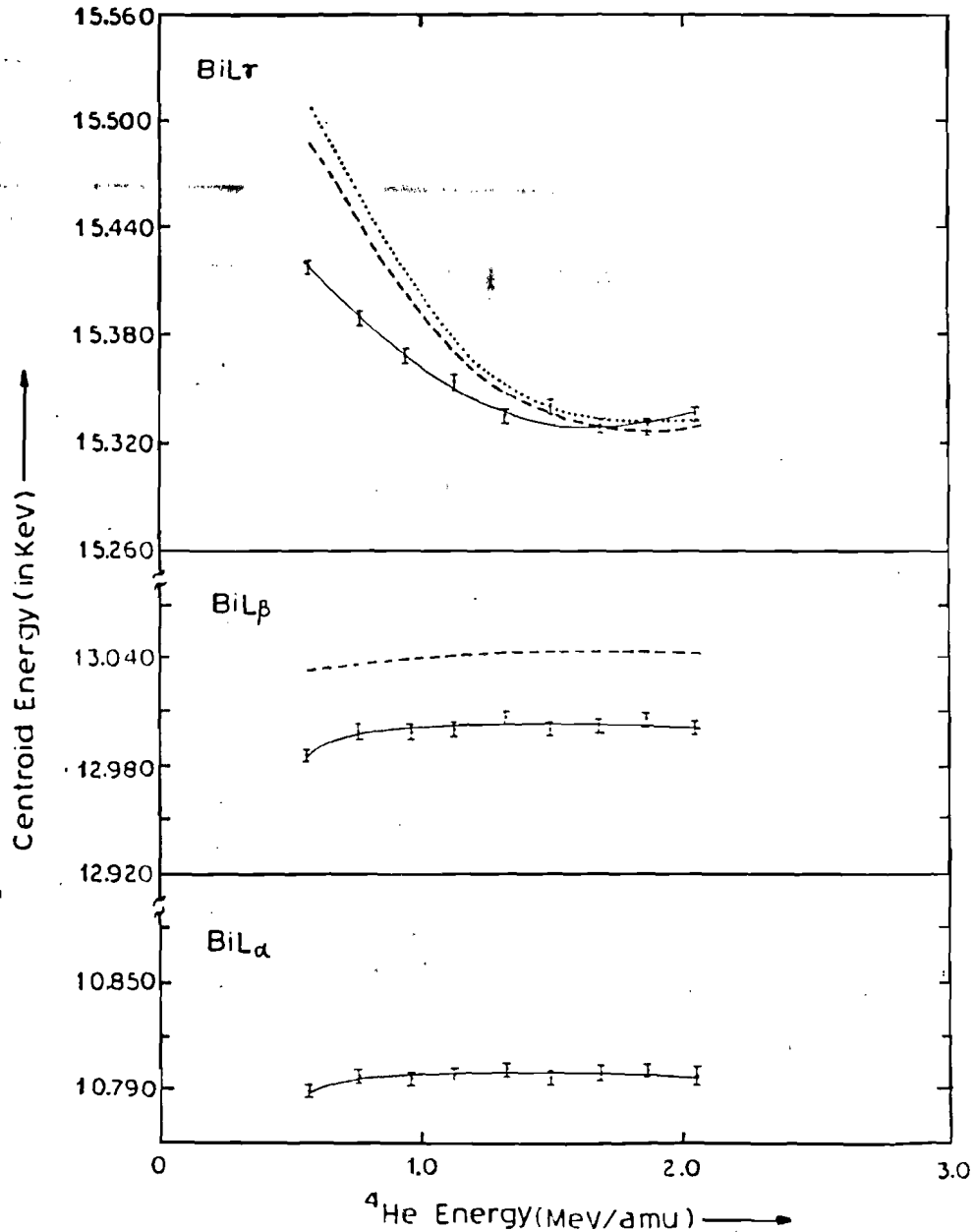
15.560
15.500
15.440
15.380
15.320
15.260
BiLτ
BiLβ
13.040
12.980
12.920
BiLα
10.850
10.790
Centroid Energy (in KeV)
0
1.0
2.0
3.0
4He Energy(MeV/amu)

Fig. 12